JOURNAL OF BACTERIOLOGY, Feb. 1991, p. 997–1003
0021-9193/91/030997-07$02.00/0
Copyright © 1991, American Society for Microbiology
Vol. 173, No. 3

Velocity Changes, Long Runs, and Reversals in the *Chromatium minus* Swimming Response

JAMES G. MITCHELL,[1,2]† MAIRA MARTINEZ-ALONSO,[1,2] JORDI LALUCAT,[3] ISABEL ESTEVE,[1,2] AND SIMON BROWN[4]

Department of Genetics and Microbiology[1] and Institute of Fundamental Biology,[2] Autonomous University of Barcelona, 08193 Bellaterra, and Department of Biology and Institute for Advanced Study, Consejo Superior de Investigaciones Científicas, University of the Balearic Islands, Palma de Mallorca,[3] Spain, and Glynn Research Institute, Bodmin, Cornwall PL30 4AU, England[4]

Received 27 August 1990/Accepted 24 November 1990

The velocity, run time, path curvature, and reorientation angle of *Chromatium minus* were measured as a function of light intensity, temperature, viscosity, osmotic pressure, and hydrogen sulfide concentration. *C. minus* changed both velocity and run time. Velocity decreased with increasing light intensity in sulfide-depleted cultures and increased in sulfide-replete cultures. The addition of sulfide to cultures grown at low light intensity (10 microeinsteins m^{-2} s^{-1}) caused mean run times to increase from 10.5 to 20.6 s. The addition of sulfide to cultures grown at high light intensity (100 microeinsteins m^{-2} s^{-1}) caused mean run times to decrease from 15.3 to 7.7 s. These changes were maintained for up to an hour and indicate that at least some members of the family *Chromatiaceae* simultaneously modulate velocity and turning frequency for extended periods as part of normal taxis.

Purple sulfur bacteria are anaerobic phototrophs that contain bacteriochlorophyll *a* and carotenoids as major pigments and oxidize hydrogen sulfide as the primary electron donor for photosynthesis. The oxidation is carried out in the periplasmic space by at least two separate pathways, one via cytochrome *c* and the other via a reverse sulfite reductase (18).

Chromatium spp. range in size from 1 to 40 μm, and motility is one of the distinguishing characteristics of the genus (27). There is now more qualitative and quantitative information on the motility of other genera of bacteria such as *Escherichia* and *Rhodobacter* (2, 22), despite the fact that early work on bacterial motility began with the large photosynthetic sulfur bacteria (8, 10, 28). These early works provide detailed description of movement in the larger *Chromatium* species, *Chromatium okenii* and *Chromatium weissii*, including reports of random walks and migration into attractant-containing capillaries (8, 28). Flagella were observed to propel cells in both directions of rotation, although the movement in one direction was short-lived and was interpreted as a shock or distress response (8, 10). This mechanism is distinct from that of the well-studied enteric bacteria such as *Salmonella typhimurium* and *Escherichia coli*, in which flagellar rotation in one direction usually randomly reorients the cell and rotation in the opposite direction propels the cell (21, 22). The bidirectional movement characteristic of *Chromatium* spp. is also different from that of other photosynthetic bacteria such as *Rhodobacter sphaeroides* (3), in which the motor rotates in only one direction, but is similar to the movement of spirochaetes and *Rhodospirillum* spp. (11). While *Rhodospirillum* spp. have been reported to change speed in response to light (9), early works on *Chromatium* spp. did not measure speed and enteric bacteria maintain constant speed.

Chemotaxis in enteric bacteria is achieved through a run and tumble mechanism in which a cell swims longer and tumbles less frequently when it is moving up a gradient of attractant than when it is moving normal to or down a gradient (5). The tumbling frequency is controlled by the interaction of the attractant (stimulus) with receptors on the cell surface. A substrate for which there is no specific processing mechanism is ignored. In contrast, members of the family *Chromatiaceae* and other bacteria change swimming speed as light intensity changes (9, 10). This has the advantage that cells may stop or almost stop under favorable conditions and so accumulate in the region where conditions are advantageous or optimal for growth. Since speed is reduced, cost to the cell is also reduced. The disadvantage of reducing speed is that gradients of physical factors present in the environment may influence speed and so cause accumulation or migration that is deleterious (7, 13, 14). Temperature, viscosity, osmotic pressure, and sulfide concentration were used here to elucidate the mechanisms by which *Chromatium minus* achieves migration in a gradient.

We found *C. minus* changed both velocity and run time. This dual system may be explained by the need of these obligate anaerobes to precisely place themselves in a vertically stratified environment, such as the band of cells in Fig. 1, so that they receive necessary light and sulfide but minimize exposure to oxygen. This precise positioning capability is reflected and supported by quantitative laboratory observations here, in previous qualitative work (8, 10, 26, 28), and in reports from field distributions (15).

MATERIALS AND METHODS

Growth media and conditions. *C. minus* was isolated by Montesinos (24) from Lake Cisó, Banyoles, Spain. Cells were grown on minimal salts medium by the method of van Gemerden and Beeftink (29) with hydrogen sulfide added daily to 1 mM unless otherwise stated. Cultivation temperature was at 23°C, and light intensity was between 20 and 30 microeinsteins (μE) m^{-2} s^{-1} unless otherwise stated.

* Corresponding author.
† Present address: Center for Microbial Ecology, 426 Giltner Hall, Michigan State University, East Lansing, MI 48824-1101.

FIG. 1. A population of *C. minus* positioning itself in a gradient of oxygen (diffusing from the surface) and sulfide (introduced at the bottom) in a 125-ml bottle. The dark band in the middle of the bottle is the cell population. The band narrows until cell concentration in the band is sufficient to start density-driven convection. The beginning of this convection can be seen at the bottom of the band as faint streamers of cells. Injection of larger amounts of sulfide moved the band upward in the bottle. The band is the macroscopic result of the behavior of individual cells, as described in the text and figure legends.

Because *C. minus* is sensitive to oxygen, care was taken to minimize the exposure of media to air. This was particularly important during microscopic examination. Cells were observed in chambers created by placing strips of coverslip on a slide and covering these with a whole coverslip. This created a chamber with a depth of 100 μm between slide and coverslip, with gaps of 1 to 3 mm at each corner. To check for wall effects, cell velocity was also measured in chambers 10 (no prop) and 1,000 (slide prop) μm deep. Chambers were filled by capillary attraction from one of the corners, while the gaps at the other three corners allowed air to escape. Samples that were to be viewed either for more than a few minutes or repeatedly were sealed at the edges with silicone stopcock grease or sterile petrolatum. This allowed cells to be viewed for hours, and cells remained motile for up to 2 weeks.

Video measurements. Measurements were made by using an Olympus BH-2 reflected light microscope at a magnification of ×400 and a Sony professional video camera for recording bacterial movement. For the video recordings an entire population of motile cells was measured. Stationary cells were not included in the counts. No attempt was made to distinguish between single cells and cells that had divided but not separated. Recordings were made on a Umatic video magnetic tape recorder, and for counting, the images were transferred to VHS format. Distance on the video screen was calibrated by recording a stage micrometer. The measured error due to screen distortion was less than 2.5%. The primary source of error appeared to be that associated with manually starting and stopping the stopwatch and with decrease in path length associated with projecting a three-dimensional process onto a two-dimensional screen (see Discussion). Measurements were made on the monitor screen by stretching plastic wrap flat against the screen surface and following a cell with a permanent marking pen (Fig. 2). This process was timed, and the same path could be rerun to check the timing. This gave values for velocity, path curvature, and reversal angle.

Direction reversals were not always exactly 180°. To measure the angle, reversals were videotaped and pathways were traced onto plastic wrap directly from the television screen. A sample is shown in Fig. 2B. Angles were measured with a protractor and checked trigonometrically.

Direct measurements. Direct measurements were made with a Nikon or an Olympus BH2 phase-contrast microscope at ×400 magnification. Velocity was measured by recording with a stopwatch the time required for a cell to swim from the center to the edge of the microscope field. Since the cells did not always swim in a straight line, this method gives an average velocity. Cells that stopped or reversed direction before reaching the edge were not counted. With this method, only one cell in a field could be measured at a time. The cells within a field showed a range of velocities. To minimize unknown or uncontrollable observer bias, the cell judged fastest in each field was the one measured. This overestimates the mean velocity of the population but was considered preferable to attempting to choose a cell moving with the mean velocity. Direct microscopic measurements were considered inferior to video-derived values, and their use was minimized. The sulfide and light experiments, in which velocity changes were pronounced, were the only ones in which direct measurements of velocity were made.

At intervals, swimming cells reversed direction. The time between these reversals was measured and was called the run time. To minimize collision with the chamber walls, which might decrease the run time, measurements were made only on cells in the center of the chamber. The center of the chamber was found by using the vernier scale on the microscope fine focusing knob. Duplicate tubes were used for each condition.

Temperature change. Chambers were sealed with silicone grease. Velocity and path curvature were measured at 5.15, 10.30, 15.40, 21.33, 25.70, 30.84, 36.36, 41.19, and 46°C on the microscope stage. The stage temperature was maintained by the Peltier effect through a computation system controlled by a personal computer with resolution and reproducibility of ±0.003 K (1). Changes between temperatures were made over 5 to 15 min, and cells were maintained at each temperature for between 5 and 10 min. During both periods the stage was maintained under a nitrogen atmosphere to prevent condensation and to further reduce exposure to oxygen.

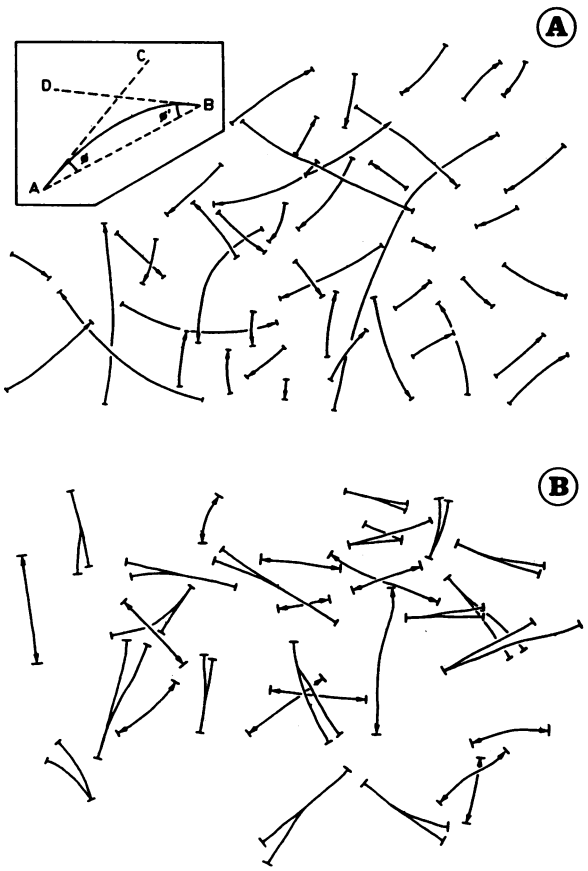

FIG. 2. Trajectories of *C. minus* as seen after being traced from the television screen onto clear plastic wrap. Each line represents the path length a cell traveled, with the arrowhead indicating the direction. (A) Velocity was calculated from the time a cell took to travel the length of the arrow. The inset shows how the path curvature was measured. A straight line was drawn from the beginning to the end of a cell path (A to B) in which there were no turns or stops. Then, tangents (AC and BD) were drawn at the beginning and ending points, creating two angles, ϕ and ϕ' (BAC and ABD), which were measured to the nearest quarter degree and averaged. The process was repeated for each path. (B) Trajectories of *C. minus* that include reversals. Double-headed arrows indicate that cells reversed and retraced the line to within the resolution of the method, between 1 and 2 μm. The angles of these reversals were counted as 180°. Lines without arrows are the sides of the reversal angle.

To increase viscosity, dextran (molecular weight, 5×10^5) was used at concentrations (wt/vol) of 0.25, 0.5, 1.1, and 2.2% or glycerol was used at concentrations of 2.5, 5, 10, and 20%. Adding glycerol increased osmotic pressure. Values for viscosity and osmotic pressure were obtained from the CRC Handbook (30). To increase sulfide concentration, neutralized sodium sulfide was added to 125-ml cultures for a final concentration of 1 mM (29), and the first velocity measurements began 3 to 7 min later. Over the next 24 h, five to seven measurements followed this first measurement. This process was repeated at 1, 10, 25, 50, and 100 μE m^{-2} s^{-1}.

Cell diffusivity. The diffusion coefficient for a population of cells was calculated from cell velocity, the run time, and the cells' reversal angle (see reference 4, p. 93). D_t is the diffusivity based on turning angle (4):

$$D_t = v^2 t/[3(1 - G)] \quad (1)$$

where v is cell velocity, t is run time, and G is the cosine of the angle. The rotational diffusion of the cell, D_r, is given as

$$D_r = kT/8\pi n a^3 \quad (2)$$

where k is Boltzmann's constant, T is absolute temperature, n is dynamic viscosity, and a is the cell radius of an equivalent sphere (measured average long radius = 2.25 μm [23a]). Equation 2 is an overestimate of diffusional rotation (D_r) that does not account for the stabilizing influence of the flagellar bundle. Correction for this stabilization is presented in the Discussion. D_r was used for calculating the time, t, it took for a cell to rotate through a given angle from reference 4:

$$t = \langle\theta^2\rangle/4D_r \quad (3)$$

where $\langle\theta^2\rangle$ is the mean-square angular displacement for a cell of rotational diffusional coefficient D_r.

RESULTS

Run times. Analysis of video tracks (Fig. 2) showed that cells, on average, reversed direction once every 7 to 20 s at 23°C and that the run time was not significantly influenced by chamber depths (Table 1). The frequency distributions of run times are shown in Fig. 3. The distributions for low (10 μE m^{-2} s^{-1}) and high (100 μE m^{-2} s^{-1}) light intensity best fit the exponential function $y = ae^{-bx}$ (Fig. 3). At low light intensity, $a = 0.23$ (standard error [SE] = 0.020), $b = 0.048$ (SE = 0.006), and $r^2 = 0.85$. At high light intensity, $a = 0.77$ (SE = 0.020), $b = 0.145$ (SE = 0.0039), and $r^2 = 0.997$. The distributions were different ($P > 0.95$).

Direction reversal. To change directions, the cells did not turn; rather, the front became the back and the back became the front (Fig. 2B). About half of all reversals were within 2° of 180°. In many runs, cells would retrace their path for 10 to 15 μm and then veer abruptly off of the path (Fig. 2B; paths without arrows), swimming along a straight line in a new direction. These deviations were included in the measurements of reversal angle, as the cells did not tumble during the veer and as the front end of the cell remained the front end. Mean reversal angles were 173.0° (95% confidence interval [CI] = 2.2°; $n = 56$) in sulfide-depleted cultures and 175° (95% CI = 1.7°; $n = 71$) in cultures with sulfide.

TABLE 1. The influence of light, chamber depth, and hydrogen sulfide on the run times of *C. minus*

Sulfide concn (mM)	Run time (s) (95% CI) (n) at the following light intensity (μE/m^2/s) and chamber depth (μm):			
	100 and 10	100 and 100	100 and 1,000	10 and 100
0	11.0 (3.7) (129)	15.3 (2.6) (55)	14.2 (1.4) (86)	10.5 (2.2) (196)
1	ND[a]	7.70 (1.6) (112)	ND	20.8 (4.1) (196)

[a] ND, Not done.

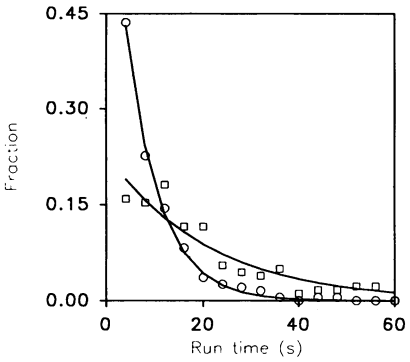

FIG. 3. The measured (symbols) and estimated (lines) probability distributions of run times for cells grown at 10 (□) and 100 (○) μE m^{-2} s^{-1}. Run times longer than 60 s are not plotted (65, 67, 68, 70, 75, 82, 84, 85, 88, 99, 115, and 131 s at 10 μE m^{-2} s^{-1}, and none longer than 60 s at 100 μE m^{-2} s^{-1}). The runs longer than 60 s represent about 6% of the 207 low-light-intensity runs measured.

Path curvature. Cells did not swim in straight lines (Fig. 2); their mean path curvatures were 5.6° (95% CI = 0.97°), 8.4° (95% CI = 0.73°), and 6.4° (95% CI = 1.4°) over 1 s at 15, 23, and 30°C. At the same temperatures the theoretical curvatures from equations 2 and 3 were 13, 14.5, and 16° over 1 s. The discrepancy between the two sets of values is explained in the discussion.

Velocity changes. Velocity increased as a function of temperature with a slope of 0.54 μm s^{-1} $°C^{-1}$ (Fig. 4A). For 1 cP of viscosity increase, velocity decreased 5.9 μm s^{-1} (Fig. 4B). For 1 osmol increase of osmotic pressure per kilogram, velocity decreased by 3.3 μm s^{-1} (Fig. 4C). The decrease in viscosity that occurred with an increase in temperature explained about 26% of the velocity increase. The remaining 74% is attributed to increased metabolic activity. Figure 4 shows that when only viscosity was changed (by using dextran) and temperature was kept constant, the velocity changed by 6 μm s^{-1} cP^{-1}, whereas the change was 23 μm s^{-1} cP^{-1} with the temperature change.

The influence of light intensity on cell velocity depended on whether sulfide was present in the medium (Fig. 5). When sulfide was present, velocity decreased by 23%. Between 10 and 100 μE m^{-2} s^{-1}, velocity decreased 23% when sulfide was present and 67% when sulfide was absent (Fig. 5).

The velocity increase caused by sulfide was transient (Fig. 6). Velocities began to decrease immediately after the sulfide was added. The decrease corresponded to the appearance and development of sulfur inclusions in the cells, which indicates a depletion of sulfide in the medium. The maximal velocity achieved after the addition of sulfide was independent of the initial background velocity. The maximal velocity did not depend on the amount of sulfide added and was the same at 0.1, 1, and 5 mM sulfide concentrations (Fig. 6B). What did change with the change in sulfide concentration was the time cells required to return to the initial velocity; the cells in 0.1 mM sulfide required minutes, while the cells in 5 mM sulfide required hours (Fig. 6B). During these periods of maximal velocities, the diffusivities were 2×10^{-5} and 0.4×10^{-5} cm^2 s^{-1} at 10 and 100 μE, respectively, with sulfide and 0.1×10^{-5} at 100 μE without sulfide.

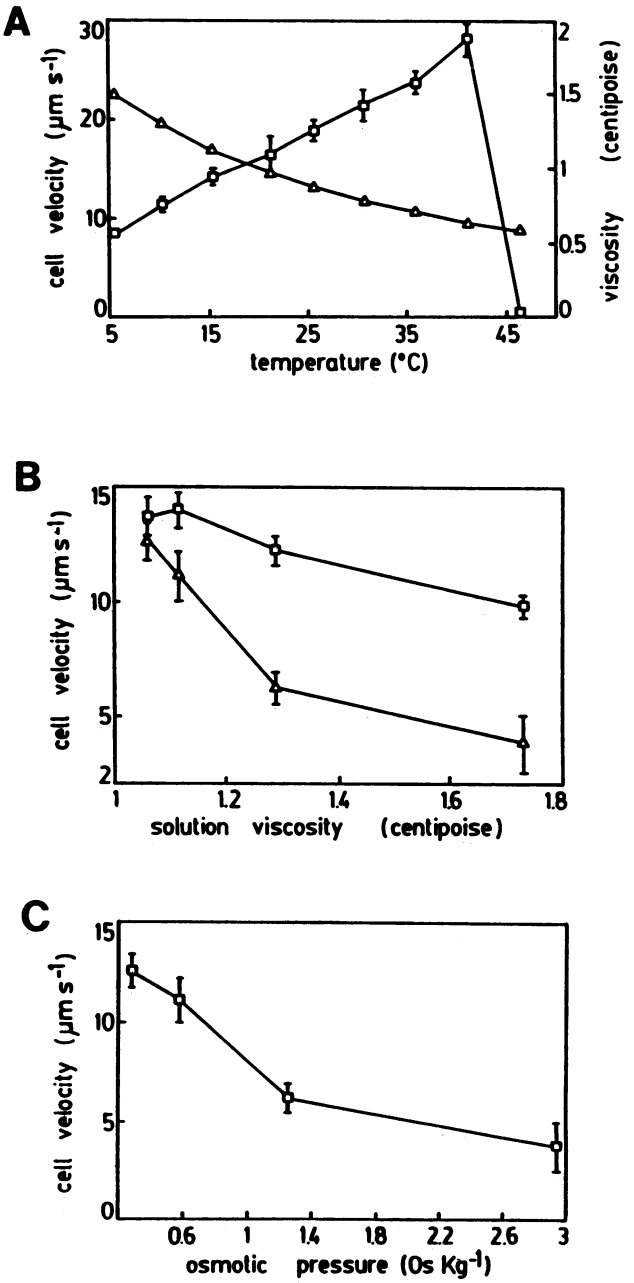

FIG. 4. The change in cell velocity as a function of the physical parameters of the medium. (A) The effect of temperature on cell velocity and viscosity. Symbols: □, cell velocity; △, viscosity of water (30). (B) Cell velocity as a function of viscosity. Symbols: □, velocity with dextran added; △, velocity with glycerol added. (C) Velocity as a function of osmotic pressure. Glycerol was used to change the osmotic pressure (see Materials and Methods). Error bars in A, B, and C are ± the 99% CI. Where there are no bars, the error is smaller than the symbol.

DISCUSSION

The motility of the purple sulfur bacterium *C. minus* is characterized by mean run times of 7 to 20 s, 180° direction reversals, and velocity that changes in response to viscosity, light, and hydrogen sulfide. These characteristics are in contrast to those of the well-studied enteric bacteria that have run times of 1 to 2 s, usually reorient by tumbling, and display uniform velocity for a given cell. As a consequence of the long run times of *C. minus*, it may be able to sense shallower gradients than enteric bacteria. Sensitivity to

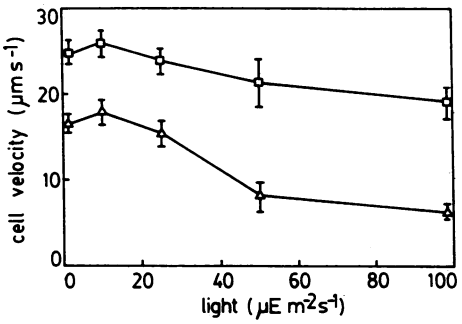

FIG. 5. The effect of cultivation conditions on cell velocity. Cells were cultivated at five different light intensities and harvested after depletion of sulfide and intracellular sulfur (no visible inclusions). The lower line represents velocities of cells incubated in the absence of sulfide, and the upper line represents cells immediately after (within 7 min) exposure to 1 mM sulfide. Symbols: △, velocities in sulfide-depleted cultures. Error bars are ± the 99% CI.

chemical gradients depends on the possession of specific receptors which recognize the compound, their number on the cell surface, and their radius. A mathematical description which predicts cell sensitivity to gradients, as a function of the gradient steepness and the aforementioned physiological characteristics, was presented by Berg and Purcell (6). By using their notation, the time, T, to sense a concentration is

$$T > \left[\pi a D\left(\frac{Ns}{Ns + \pi a}\right)\left(\frac{\bar{c}c_{1/2}}{\bar{c} + c_{1/2}}\right)\left(\frac{1}{\bar{c}}\frac{\partial \bar{c}}{\partial t}\right)^2\right]^{-1/3} \quad (4)$$

where a is cell radius, D is molecular diffusivity, N is the number of receptors on the cell surface, s is the receptor radius, $\bar{c}$ is the mean concentration, $c_{1/2}$ is the ligand concentration at which half of the receptors are bound, and $(1/\bar{c})$ $(\partial\bar{c}/\partial t)$ is the temporal gradient. The temporal gradient is converted to a spatial gradient by substituting $(v/\bar{c})$ $\partial\bar{c}/\partial x$ (6), where v is cell velocity. We define a binding constant as

$$B = \pi a D\bar{c}\,[Ns/(Ns + \pi a)] \quad (5)$$

To change the inequality in equation 4 to an equality, we define the dimensionless empirical constant K, which relates the minimum time needed for sensing the gradient to the time over which solutes diffuse to the receptors. Substituting equation 5 in equation 4 and rearranging gives

$$\frac{\partial \bar{c}}{\partial x} > [\bar{c}^2(\bar{c} + c_{1/2})/T^3Bv^2c_{1/2}]^{1/2} \quad (6)$$

Equation 6 predicts that as run time increases, progressively shallower gradients can be detected. Thus, *C. minus* is well adapted to sense shallow environmental gradients.

Path curvature correction and significance. Longer run times only function as a strategy to detect shallow gradients if during the run the cell is not deflected more than about 90° by Brownian motion. For this reason, the angles of the path curvatures were measured. The observed values (5.6, 8.4, and 6.4° in 1 s) must be corrected for the reduction in curvature that results from tracing a three-dimensional path onto a two-dimensional surface. The values, corrected for this loss, are 7.9, 11.9, and 9.0° in 1 s. The theoretical curvatures obtained from equations 2 and 3 (13, 14.5, and 16° in 1 s) depend on cell size, temperature, and viscosity and need to be corrected for the stabilization against rotation provided by the flagellar bundle. The equation for rotational

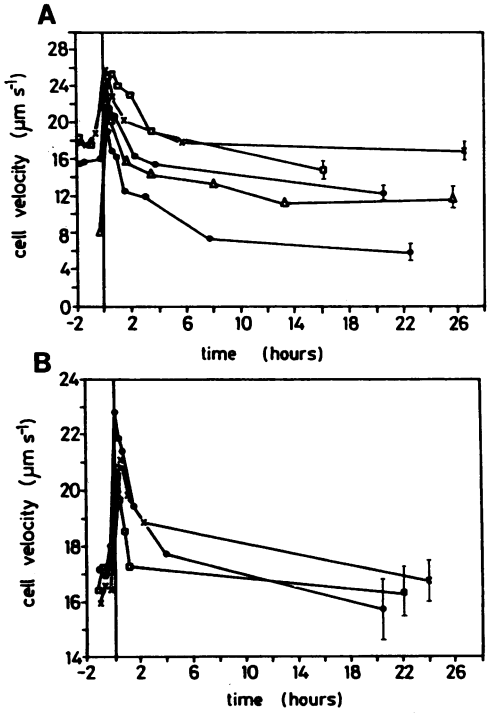

FIG. 6. Cell velocity as a function of time. At time zero, sulfide was added to 1 mM. Cells were grown at 25 μE m^{-2} s^{-1}. Values before time zero are measurements in sulfide-depleted cultures in which cells contained no visible sulfur inclusions. (A) Each line represents cells grown at different light intensities: 100 (●), 50 (○), 25 (△), 10 (x), and 1 (□) μE m^{-2} s^{-1}. (B) Effect of different concentrations of sulfide on velocity, 0.1 (□), 1 (○), and 5 (x) mM. Inclusions began appearing 15 to 30 min after the sulfide had been added to cultures. During the 10 min required for each count, there was no change in cell velocity. Error bars for A, B, and C are ± 99% CI and are approximately the same size for all points on a line. Where they are not present, they have been left off to increase the clarity of the figure.

stabilization is derived from considering the flagellar bundle as a series of small connected spheres (12) and is

$$D_r = (kT/8\pi na^3)[1 + (L/2a)]^{-3} \times \left(1 + \sum_{i=1}^{3}\sum_{j=1}^{3} b_{ij}\{1 - [1 + (L/2a)]^{-1}\}^i (a_f/a)^j\right) \quad (7)$$

where L is flagellar bundle length, b_{ij} are the rotation coefficients, a_f is the flagellar bundle radius, and other variables are as previously defined.

Solving equation 7 using nine coefficients (12) indicates that stabilization reduces rotation to 2.2, 2.5, and 2.8° in 1 s at 15, 23, and 30°C. The discrepancy between the observed and measured values may result from an incorrect assumption about flagellar bundle length, errors in measuring cell size, nonspherical cell shape, and helical swimming paths that were mistakenly measured as rotation. Alternatively, the model on which equation 7 is based may not be entirely appropriate in this case. The mean change in direction during runs of an *E. coli* wild-type strain has been measured as about 23° for a run time of about 0.9 s (5). Another work gives the rotation for *E. coli* over 1 s as about 27° and the rotation for an equivalent volume sphere (no flagellar stabilization) as about 30° (4). We calculate that an equivalent

volume *E. coli* sphere rotates between 28 and 29° in 1 s. Applying equation 7 for flagellar stabilization gives a rotation of 6.4° in 1 s. This indicates that equation 7 overestimates the stabilizing influence of the flagellar bundle on cell rotation. Our mean observed rotation of less than 10° is intermediate between the 2.5 and 15° mean theoretical rotations found above and may reflect a number close to the true rotation for *C. minus*. In any case, a curvature of a few to 10° in 1 s for *C. minus* is less than the 30° in 1 s for *E. coli* (4, 5) and means that *C. minus* can swim for more than 45 s before rotating 90°.

Run time and diffusivity. The exponential distribution of run times (Fig. 3) is consistent with previous work (5) and meets one of the requirements for using equation 1 (see reference 4). The distributions in Fig. 3 indicate that reversal is more frequent at low light intensity than at high light intensity. This difference persisted for minutes to hours and thus is distinct from the classical shock response reported for members of the family *Chromatiaceae* (10, 28). These longer run times and higher velocities at low light intensity increase diffusion coefficients compared with high light conditions and enhance tactic response by rapidly bringing cells into new environments to which they can respond, as is apparently occurring in Fig. 1.

Figure 3 suggests that the molecular memory of *C. minus* should be longer than in enteric bacteria. If run times in *C. minus* are controlled by methylating chemotaxis proteins or equivalent transducers, the longer memory might be explained by slower methylation and demethylation or a more extensive pool of sites and receptors than is found in enteric bacteria (16, 19).

Velocity change. Modulation of velocity appears to be controlled by at least two factors. Light decreases velocity, but exposure to sulfide overrides the decrease, raising the velocity to a maximum. A clue to the cause of this maximum is provided by the transitory nature of the velocity maximum that *C. minus* showed in response to sulfide addition. This may have been because the sulfide was added once, so that as uptake by cells occurred, the concentration in the medium decreased. This implies that velocity depended on the external concentration of sulfide and that as concentration fell so did velocity. The velocity decrease continued until a lower limit was reached. The lower velocity limit appeared to be determined by light intensity, with high light intensity depressing the minimum velocity (Fig. 6B). From this we conclude that the external sulfide concentration determines the cell velocity above a lower limit set by the intensity of light during cultivation. The light intensity probably sets the lower limit by controlling the number of reaction centers and light harvesting units. After cultivation in dim light, the number of reaction centers and light harvesting units would increase and consequently, the minimum velocity would increase. Other schemes are possible, but this may be the simplest.

Among the factors upon which the upper limits of velocity depend are the amount of thrust the flagella produce and the viscosity of the medium. The number of motors does not change over short periods, and viscosity is uniform in cultures and many environments, since it is primarily a function of temperature and secondarily a function of the medium's chemical composition. Under such constant environmental conditions, one of the important influences on velocity will be the motor rotation rate, which in turn is influenced by the proton motive force, among other factors. If the sulfide oxidation occurs in the periplasmic space, as has been proposed for members of the family *Chromatiaceae* (17, 18), protons would be added to the proton pool, which would increase motor rotation rate and give a boost to velocity. Velocity would slow as the sulfide in the medium was depleted, as we found in Fig. 6. This does not mean the cell slows because of a depletion of electron donors; the elemental sulfur in the inclusions can still donate electrons. Rather, the velocity decrease is consistent with the possibility that the two hydrogen atoms on the sulfide are removed just outside the cell membrane and subsequently diffuse down the proton gradient into the cell. The physiological limits are then the speed at which protons can be generated and the speed at which they can diffuse down their gradient. As temperature and hence molecular diffusivity increased, so did velocity, as would be expected. Physiological limits, however, do not explain the entire velocity change. The external physical environment must also be considered.

Lowe et al. (20) and Maeda et al. (23) found velocity changes with temperature for *Streptococcus* sp. and *E. coli* that were similar to those shown in Fig. 4; however, the slope in Fig. 4 at 0.5 $\mu m\ s^{-1}\ °C^{-1}$ is lower than their slopes of approximately 0.9 and 1.9 $\mu m\ s^{-1}\ °C^{-1}$, indicating a weaker dependence of velocity on temperature for *C. minus* than for *Streptococcus* sp. and *E. coli*. Figure 4C indicates that the decreased sensitivity to temperature was a metabolic response and not simply due to the reduction of drag over the cell surface. Insensitivity to temperature change makes sense for bacteria found in environments where fluctuations are large compared with the constant 37°C of the intestine.

The sensitivity of members of the family *Chromatiaceae* to sulfide is greater than for other groups that utilize sulfide such as members of the family *Chlorobiaceae* (26). Such sensitivity means that the possession of both tactic and kinetic capabilities is important for precise positioning at the interface between oxygen-rich and sulfide-rich environments (Fig. 1). The gradients in these environments, such as light, sulfide, and oxygen, are usually one-dimensional and oriented perpendicular to the acceleration of gravity, which is to say that by and large the change in a physical parameter is much greater vertically than horizontally. Corresponding vertical orientation by some *Chromatium* species can be inferred from the organized vertical migrations (25) and can be seen in the film by Pfennig (24a). The cause of such orientation is due to a combination of the hydrodynamic effect resulting from a thin tail being attached to a rod or sphere and the absence of immediate random reorientation. Vertical orientation combined with the reversal of direction, instead of random reorientation, indicates that some members of the family *Chromatiaceae* are well adapted for migrating one-dimensionally.

ACKNOWLEDGMENTS

We thank J. Adler for the translation of the Engelmann paper, I. Thorey for translation of the Buder and Rothert papers, and A. Amengual and V. Torra of the Physics Department of the University of the Balearic Islands, Mallorca, Spain, for access to their microscope and temperature-controlled stage and video system. J.G.M. thanks the UAB Genetics and Microbiology Department and its chairman R. Guerrero for acting as host and providing access to the VCR. I. Thorey, R. deWit, P. Poole, J. Armitage, C. Carrera, J. Mas, C. Pedrós-Alió, N. Gaju, and two anonymous reviewers provided valuable discussion and comments on the manuscript. Figures were drafted by J. Manuel Cuartero. V. Pavón and M. Algueró provided assistance with culturing.

Support was provided by a NASA PBI (J.G.M.), by a Spanish Ministry of Education fellowship (J.G.M.), by the Center for Micro-

bial Ecology (J.G.M.), and by CICYT PB 87-0500 (I.E.) and MAR88-0225 (J.L.).

REFERENCES

1. **Amengual, A., and V. Torra.** 1989. An experimental set-up for thermal analysis and DSC. Its application to the hysteresis cycles in shape memory alloy. J. Phys. E Sci. Instrum. **22**(7): 433–437.
2. **Armitage, J. P.** 1989. Tactic responses in photosynthetic bacteria. Can. J. Microbiol. **34**:475–481.
3. **Armitage, J. P., and R. M. Macnab.** 1987. Unidirectional, intermittent rotation of the flagellum of *Rhodobacter sphaeroides*. J. Bacteriol. **169**:514–518.
4. **Berg, H. C.** 1983. Random walks in biology. Princeton University Press, Princeton, N.J.
5. **Berg, H. C., and D. A. Brown.** 1972. Chemotaxis in *Escherichia coli* analysed by three-dimensional tracking. Nature (London) **239**:500–504.
6. **Berg, H. C., and E. M. Purcell.** 1977. Physics of chemoreception. Biophys. J. **20**:193–219.
7. **Berg, H. C., and L. Turner.** 1979. Movement of microorganisms in viscous environments. Nature (London) **278**:349–351.
8. **Buder, J.** 1915. Zur Kenntnis des *Thiospirillum jenense* und seiner Reaktionen auf Lichtreize. Jahrb. Wiss. Bot. **56**:529–584.
9. **Clayton, R. K.** 1958. On the interplay of environmental factors affecting taxis and motility in *Rhodospirillum rubrum*. Arch. Mikrobiol. **29**:189–212.
10. **Engelmann, T. W.** 1883. *Bakterium photometricum*. Ein Beitrag zur vergleichenden Physiologie des Licht- und Farbensinnes. Pfluegers Arch. Gesamte Physiol. Menschen Tiere **42**:183–186.
11. **Fosnaugh, K., and E. P. Greenberg.** 1988. Motility and chemotaxis of *Spirochaeta aurantia*: computer-assisted motion analysis. J. Bacteriol. **170**:1768–1774.
12. **Garcia de la Torre, J., and V. A. Bloomfield.** 1981. Hydrodynamic properties of complex, rigid, biological macromolecules: theory and applications. Q. Rev. Biophys. **14**:81–139.
13. **Gotz, R., N. Limmer, K. Ober, and R. Schmitt.** 1982. Motility and chemotaxis in two strains of *Rhizobium* with complex flagella. J. Gen. Microbiol. **128**:789–798.
14. **Greenberg, E. P., and E. Canale-Parola.** 1977. Motility of flagellated bacteria in viscous environments. J. Bacteriol. **132**: 356–358.
15. **Guerrero, R., E. Montesinos, C. Pedrós-Alió, I. Esteve, J. Mas, H. van Gemerden, P. A. G. Hofman, and J. F. Bakker.** 1985. Phototrophic sulfur bacteria in two Spanish lakes: vertical distribution and limiting factors. Limnol. Oceanogr. **30**(5):919–931.
16. **Hazelbauer, G. L., C. Park, and D. M. Nowlin.** 1989. Adaptional "crosstalk" and the crucial role of methylation in chemotactic migration by *Escherichia coli*. Proc. Natl. Acad. Sci. USA **86**:1448–1552.
17. **Hooper, A. B., and A. A. DiSpirito.** 1985. In bacteria which grow on simple reductants, generation of a proton gradient involves extracytoplasmic oxidation of substrate. Microbiol. Rev. **49**: 140–157.
18. **Kelly, D. P.** 1988. Oxidation of sulfur compounds, p. 65–98. *In* J. A. Cole and S. J. Ferguson (ed.), The nitrogen and sulfur cycles. Cambridge University Press, Cambridge.
19. **Koshland, D. E.** 1977. A response regulator model in a simple sensory system. Science **196**:1055–1063.
20. **Lowe, G., M. Meister, and H. C. Berg.** 1987. Rapid rotation of flagellar bundles in swimming bacteria. Nature (London) **325**: 637–640.
21. **Macnab, R. M.** 1977. Bacterial flagella rotating in bundles: a study in helical geometry. Proc. Natl. Acad. Sci. USA **74**:221–225.
22. **Macnab, R. M.** 1987. Motility and chemotaxis, p. 732–759. *In* F. C. Neidhardt, J. L. Ingraham, K. B. Low, B. Magasanik, M. Schaechter, and H. E. Umbarger (ed.), *Escherichia coli* and *Salmonella typhimurium*: cellular and molecular biology, vol. 1. American Society for Microbiology, Washington, D.C.
23. **Maeda, K., Y. Imae, J.-I. Shioi, and F. Oosawa.** 1976. Effect of temperature on motility and chemotaxis of *Escherichia coli*. J. Bacteriol. **127**:1039–1046.

23a. **Martínez-Alonso, M.-R.** 1988. M.S. thesis. Autonomous University of Barcelona, Barcelona, Spain.

24. **Montesinos, E.** 1987. Change in size of *Chromatium minus* cells in relation to growth rate, sulfur content, and photosynthetic activity: a comparison of pure cultures and field populations. Appl. Environ. Microbiol. **53**:864–871.

24a. **Pfennig, N.** 1966. *Chromatium okenii* (Thiorhodaceae) Biokonvektion, aero- und phototaktisches Verhalten. Videokassette E1036. Institut für den Wissenschaftlichen Film, Göttingen, Germany.

25. **Pfennig, N.** 1962. Beobachtungen uber das Schwarmen von *Chromatium okenii*. Arch. Mikrobiol. **42**:90–95.
26. **Pfennig, N.** 1967. Photosynthetic bacteria. Annu. Rev. Microbiol. **21**:285–324.
27. **Pfennig, N., and H. G. Trüper.** 1974. Order I. *Rhodospirillales* Pfennig and Trüper 1971, 17, p. 24–25. *In* R. E. Buchanan and N. E. Gibbons (ed.), Bergey's manual of determinative bacteriology, 8th ed. The Williams & Wilkins Co., Baltimore.
28. **Rothert, W.** 1901. Beobachtungen und Betrachtungen uber taktische Reizerscheinungen. Flora **88**:371–421.
29. **van Gemerden, H., and H. H. Beeftink.** 1983. Ecology of phototrophic bacteria, p. 146–185. *In* J. G. Ormerod (ed.), The phototrophic bacteria: anaerobic life in the light. Blackwell Scientific Publications Ltd., Oxford.
30. **Weast, R. C.** 1975. The handbook of chemistry and physics, 56th ed. CRC Press, Cleveland.